SHALLOW-SEISMIC WAVEFIELD SCATTERING AND IMPLICATIONS FOR VISCOELASTIC FWI

N. Athanasopoulos, T. Bohlen

email: *nikolaos.athanasopoulos@kit.edu*
keywords: *shallow scattering, surface waves, full-waveform inversion*

ABSTRACT

The aim of this study is to investigate the seismic response from shallow structures using a 2D finite-difference method. Full-waveform inversion (FWI) suffers from so-called cross-talk between viscoelastic parameters, i.e. certain combinations of viscoelastic parameters have the same scattering signature. We evaluate the scattering response from individual perturbations in the viscoelastic material parameters. By subtracting a perturbed from a background medium and solving the viscoelastic wave equation we obtain the scattering wavefield. Additionally, we evaluate the instantaneous energy density of P- and S-waves to better understand the influence of scattering. This allows us to provide some fundamental insights into the composition of seismic recordings and ideas of how to mitigate cross-talk in shallow-seismic applications of FWI. Specifically, we find that the P-wave velocity structure is constrained similarly by Rayleigh, P- and S-waves. The S-wave velocity is the most reliable parameter to invert for from FWI of surface waves due to their large amplitudes. The scattering pattern of density differs fundamentally from those of velocities and attenuation. Finally, cross-talk between attenuation and velocity for both P- and S-waves is caused by the similarity of their corresponding scattering responses.

INTRODUCTION

Near-surface shallow seismics has risen in interest for engineering and geotechnical investigations. With the improvements in computational resources, full-waveform inversion (FWI) has become an attractive method not only for exploration and global scale, but also to retrieve viscoelastic multiparameter models to characterize properties of shallow structures within the first 10-20 m depth. Recent FWI applications revealed that FWI suffers from so-called cross-talk between viscoelastic parameters: certain combinations of viscoelastic parameters may cause a similar seismic response and can therefore not be discriminated, even with FWI. The aim of this study is to investigate the seismic response for a shallow structure by a series of numerical experiments using a 2D finite-difference method for solving the viscoelastic wave equation. As shallow seismic waves are dominated by surface waves we mainly analyze the scattering of surface to body waves and vice versa. This modeling study gives fundamental insights into the composition of seismic recordings and provides ideas to mitigate cross-talk in future applications of FWI.

THEORY - ELASTIC WAVE EQUATION OF THE SCATTERED WAVEFIELD

In this study we consider wave propagation in an isotropic viscoelastic medium based on the generalized standard linear solid (Carcione et al., 1988; Robertsson et al., 1994; Bohlen, 2002):

$$\partial_t v_i - \frac{1}{\rho}\partial_j \sigma_{ij} - s_i = 0, \tag{1}$$

$$\partial_t \sigma_{ij} - \lambda_0 \partial_k v_k \delta_{ij} - \mu_0(\partial_j v_i + \partial_i v_j) - r_{ij\ell}\delta_\ell - s_i = 0 \quad \text{and} \tag{2}$$

$$\partial_t r_{ij\ell} + \frac{1}{\tau_{\sigma\ell}}[\lambda_\ell \partial_k v_k \delta_{ij} + \mu_\ell(\partial_j v_i + \partial_i v_j) + r_{ijl}] = 0, \tag{3}$$

where v is the particle velocity vector, σ is the stress tensor, s is the source term, ρ is the mass density, δ_{ij} the Kronecker delta, λ and μ are the Lamé parameters (where the index 0 stands for unrelaxed and ℓ for relaxed) and r is the memory variable for L Maxwell bodies with relaxation time $\tau_{\sigma\ell}$. The first equation is the equation of motion stating that the momentum of the medium, the product of density ρ and the displacement velocity v, can be changed by surface forces, described by the stress tensor σ_{ij}, or body forces s_i. Equations 2 and 3 state the contributions of the material properties, describing how the medium reacts when a certain force is applied, as well as the anelastic behavior of the medium expressed by the attenuation of seismic waves.

In the following, we numerically solve equations 1-3 with 2D finite-difference modeling, using two different models: a background and a perturbed model as shown in figure 1. We perturb the P- and S- wave velocities (v_p and v_s, rrespectively), the density (ρ), the quality factors q_p and q_s as follows :

$$v_p' \rightarrow v_p + \delta v_p, \quad v_s' \rightarrow v_s + \delta v_s, \quad \rho' \rightarrow \rho + \delta\rho, \quad q_p' \rightarrow q_p + \delta q_p \quad \text{and} \quad q_s' \rightarrow q_s + \delta q_s \tag{4}$$

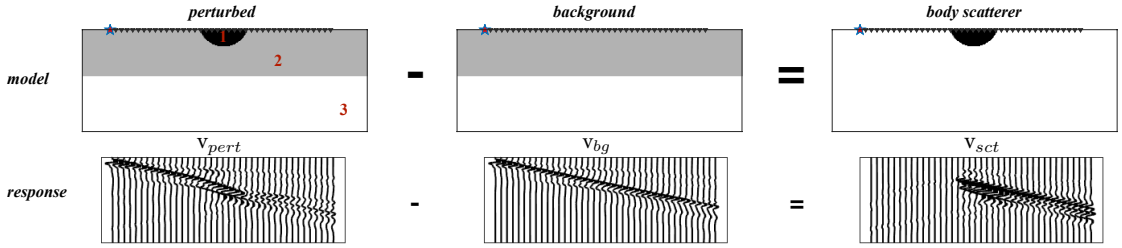

Figure 1: Sketch of the proposed methodology. Retrieval of the scattering response of a shallow structure by subtracting the seismic response of the background model.

Each time we perturb only one of the viscoelastic parameters to study its individual contribution to the recorded data. By subtracting the perturbed wavefield, $\mathbf{v}_{pert}$, from the background wavefield, $\mathbf{v}_{bg}$, we obtain the viscoelastic wave equation of the scattered wavefield, $\mathbf{v}_{sct}$, for each of the five cases shown in equation 4, given by:

$$\mathbf{v}_{\mathrm{sct_i}} = \mathbf{v}_{\mathrm{pert_i}} - \mathbf{v}_{\mathrm{bg_i}} \quad \text{where} \quad \mathrm{i} = v_p, v_s, \rho, q_p \quad \text{or} \quad q_s. \tag{5}$$

A perturbation in a material parameter acts as a secondary source producing a wavefield that we refer to as *scattered* wavefield or response (figure 1).

INSTANTANEOUS ENERGY DENSITY OF P- AND S-WAVES

Every vector field can be decomposed into a rotation-free and a divergence-free part. Since the divergence of a curl and the rotation of a divergence are zero, we get two independent equations which correspond to the viscoelastic wave equation for the propagation of compressional ($\nabla \cdot \mathbf{v}$) and shear ($\nabla \times \mathbf{v}$) waves (Morse and Feshbach, 1953). The vector product $\nabla \times \mathbf{v}$ corresponds to a rotation, describing a change of shape without any volume change, i.e. pure shearing, while the term $\nabla \cdot \mathbf{v}$ describes a volume change (compression and dilatation), which also contains some rotation-free shearing (except for hydrostatically compressed media). We can then define the instantaneous energy density (or intensities) for P- and S-wave

particle velocities (E_p and E_s, respectively) in 2D by:

$$\mathrm{E_p} = \sqrt{\lambda + 2\mu}(\nabla \cdot \mathbf{v}) = \sqrt{\lambda + 2\mu} \cdot (\partial_\mathrm{x} \mathrm{v_x} + \partial_\mathrm{y} \mathrm{v_y}) \quad \text{and} \tag{6}$$

$$\mathrm{E_s} = \sqrt{\mu}(\nabla \times \mathbf{v})_\mathrm{z} = \sqrt{\mu} \cdot (\partial_\mathrm{x} \mathrm{v_y} - \partial_\mathrm{y} \mathrm{v_x}). \tag{7}$$

In the above statement, we have preserved the divergence and curl sign information, while showing relative compressional and shear energy amplitudes similar to Dougherty and Stephen (1988). In the next section, we will use these principles to provide snapshots of the background and scattered wavefields based on the numerical solutions of shallow seismic scattering from body and surface waves.

RESULTS

We examine the effects of near-surface heterogeneities on the recorded waveforms by simulating equations 1-3 using the background, perturbed and scattered models for each parameter as shown in figure 1. The acquisition geometry of the study consists of a linear profile of 39 vertical geophones with an equidistant spacing of 1 m, and we use a vertical source with dominant frequency of 30 Hz. Both receivers and sources are located at the surface, both to recreate a realistic scenario and to study surface-to-surface scattering which is of great interest for our case. The size of the model we examine is 50 by 18 m, where we use two homogeneous half-spaces with a discontinuity separating them at a depth of 8 m (figure 1). The body scatterer is located at the surface and it bears a semi-circular shape with dimensions 9 m (horizontal) by 3 m (vertical). The values for each layer and the surface structure (scatterer) for the elastic parameters are shown in table 1 and are chosen to correspond to previous synthetic FWI studies that we performed (Wittkamp et al., 2019).

	v_p (m/s)	v_s (m/s)	ρ (kg/m^3)	$q_\mathrm{p}/q_\mathrm{s}$ $(\cdot)$
1: body scatterer	355 (-23%)	92 (-45%)	1500 (-12%)	20 (-60%)
2: top layer	460	165	1700	50
3: bottom layer	1745	275	2000	200

Table 1: Material properties of the models shown in figure 1. The percentage of reduction from the background model is shown as well.

The results are summarized in figure 2. The wavefield of the background medium is shown in figure 2a.1-3. The wavefield is dominated by the Rayleigh wave which has a strong component of S-wave intensity (E_s, figure 2a.1) and weak P-wave contribution (E_p, figure 2a.2), also shown in the recorded shot gather.

Perturbation in v_p $(-23\ \%)$, figure 2b: The scattered wavefield has similar intensity for both P- and S-waves. Mainly forward scattering into the direction of the Rayleigh wave occurs. A relatively high back-scattering intensity of P-waves is also observed. The recorded seismic response at the surface is composed of forward scattered P- and S-waves and surface waves. This indicates that both the coda of the first arrival and the Rayleigh wave may contribute similarly to update the P-wave velocity model during FWI. Its amplitude, however, is small compared to the reference, revealing the difficulty of retrieving accurate P-wave velocities while using least-squares inversion schemes. Hierarchical approaches using time-windowing can therefore improve the reconstruction of P-wave velocity (Athanasopoulos et al., 2018).

Perturbation in v_s $(-45\ \%)$, figure 2c : The scattering response due to an S-wave velocity perturbation is dominated by Rayleigh-wave scattering into the forward direction. The amplitudes of the forward scattered Rayleigh wave are comparable to the amplitude of the direct Rayleigh wave (figure 2a). This indicates that FWI of Rayleigh waves is most sensitive to shallow S-wave perturbations, i.e. a reliable reconstruction of the S-wave velocity model can be achieved.

Perturbation in ρ $(-12\ \%)$, figure 2d : The scattering response due to density perturbation differs fundamentally from perturbations in seismic velocities and attenuation. We can observe a surprisingly strong back-scattering of P- and especially S-waves caused by both the direct P- and Rayleigh wave. In particular the intensity of S-waves shows that the back-scattered energy is almost half the intensity of the forward

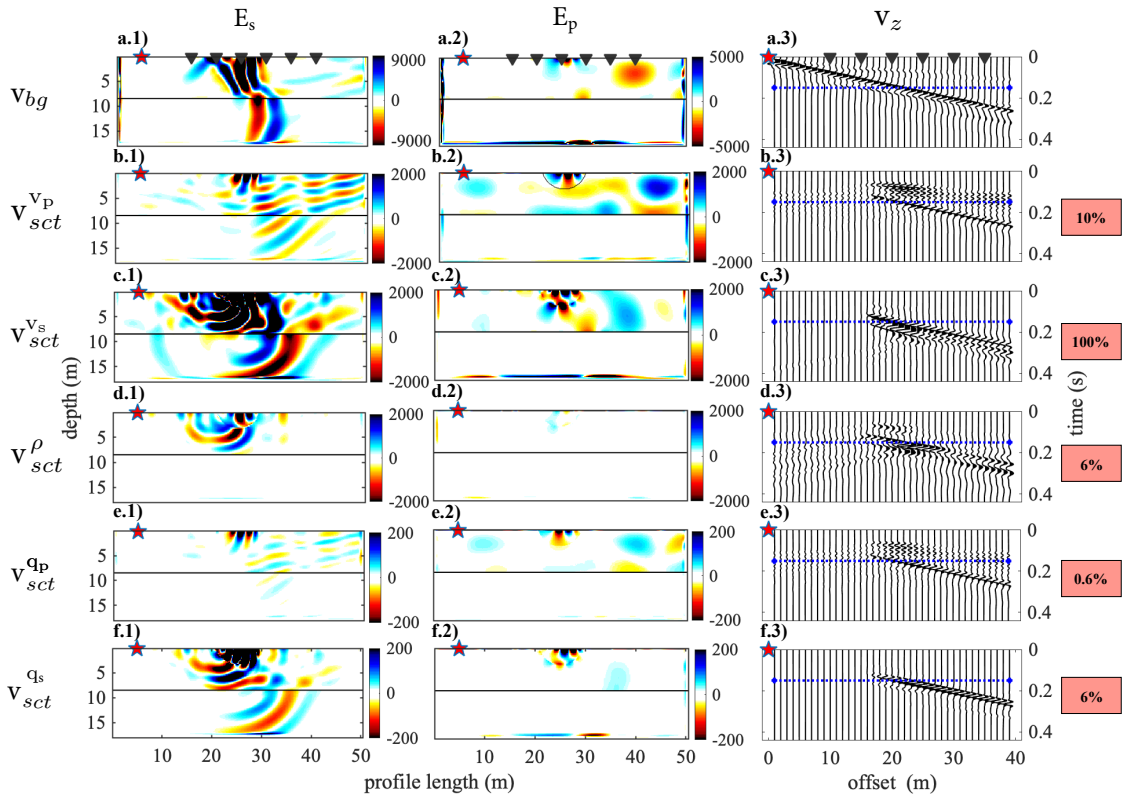

Figure 2: Snapshots of the S-wave (E_s) and P-wave (E_p) intensity of the background wavefield (top row) and scattered wavefields caused by perturbations of the viscoelastic parameters (table 1). The corresponding seismic response of particle velocity is shown in the right column. Triangles mark the positions of some reference receivers and stars indicate the shot location. For better visualization the amplitudes of the scattered wavefield are clipped to lower values as indicated by the colorbars. The boxes signify the reduction in percentage of the amplitudes of the shot gathers compared to the background (a.3).

scattering. This shows that separating forward and back-scattered waves in FWI (with an FK-filter one can invert separately the positive and negative wavenumbers) could potentially improve the reconstruction of density models. However, we observe that the amplitude of a density perturbation constitutes a change of only 6 % relative to the reference recordings making density especially challenging to invert for in FWI.

Perturbation in q_p and q_s (-60 %), figures 2e and 2f : The scattered wavefield due to perturbations in attenuation of P- and S-waves is similar to the intensities of the respective velocity perturbations (figures 2b and 2c). This indicates that the velocity dispersion caused by attenuation controls the scattering behavior. Amplitude loss is negligible here due to the small size of the structure (body scatterer). Due to the similarity of the scattering responses and intensities of velocities and attenuation we can expect a significant cross-talk between v_p-q_p and v_s-q_s, making q_p and q_s the most challenging parameters to invert for. This effect may be reduced by accounting for frequency-dependent amplitude decay due to attenuation, which is not considered in figure 2.

CONCLUSIONS

The numerical study of the scattering response of perturbations, caused by a shallow structure, revealed some fundamental insights into the relative contribution of scattered waves in shallow seismic recordings. These findings may be used in future applications of FWI to resolve certain material parameters and to mitigate cross-talk. Information of the shallow P-wave velocity structure is constrained in both the forward and scattered P- and S-waves, as well as the surface wave to a similar amount. Cross-talk could be reduced

by time-windowed FWI. The S-wave velocity is the most reliable parameter to invert for from FWI of surface waves due to the large amplitudes of scattered Rayleigh waves. Although the scattering response due to a perturbation in density is weak, the scattering pattern differs fundamentally from velocities and attenuation. This indicates that density reconstruction from shallow seismics suffers less from cross-talk compared to exploration seismics. Cross-talk between attenuation and velocity for both P- and S-waves is caused by the similarity of the corresponding scattering responses. This cross-talk may be reduced by incorporating the amplitude loss with offset caused by attenuation during FWI.

ACKNOWLEDGMENTS

This work was financially supported by the sponsors of the Wave Inversion Technology (WIT) Consortium. The simulations were performed on the computational resource Institutscluster II funded by participating KIT institutes and the DFG. The authors gratefully acknowledge the computing time granted on the supercomputer JUWELS at Jülich Supercomputing Centre (JSC).

REFERENCES

Athanasopoulos, N., Manukyan, E., Bohlen, T., and Maurer, H. (2018). Accurate reconstruction of shallow p-wave velocity model with time-windowed elastic full-waveform inversion. In *80th EAGE Conference & Exhibition 2018*. EarthDoc.

Bohlen, T. (2002). Parallel 3-d viscoelastic finite difference seismic modelling. *Computers & Geosciences*, 28(8):887–899.

Carcione, J. M., Kosloff, D., and Kosloff, R. (1988). Wave propagation simulation in a linear viscoelastic medium. *Geophysical Journal International*, 95(3):597–611.

Dougherty, M. E. and Stephen, R. A. (1988). Seismic energy partitioning and scattering in laterally heterogeneous ocean crust. *pure and applied geophysics*, 128(1):195–229.

Morse, P. and Feshbach, H. (1953). Methods of theoretical physics. *McGraw-Hill Book Company, New York*.

Robertsson, J. O. A., Blanch, J. O., and Symes, W. W. (1994). Viscoelastic finite-difference modeling. *Geophysics*, 9(59):1444–1456.

Wittkamp, F., Athanasopoulos, N., and Bohlen, T. (2019). Individual and joint 2-d elastic full-waveform inversion of rayleigh and love waves. *Geophysical Journal International*, 216(1):350–364.